

# Multiple occupancy considerations for the SmartPET imaging system

Toby E. Beveridge<sup>a,\*</sup>, John E. Gillam<sup>a</sup>, Andrew J. Boston<sup>d</sup>, Helen C. Boston<sup>d</sup>, Reynold J. Cooper<sup>d</sup>, Andrew R. Mather<sup>d</sup>, Chris J. Hall<sup>c</sup>, Paul J. Nolan<sup>d</sup>, Robert A. Lewis<sup>a,b</sup>

<sup>a</sup>*School of Physics, Monash University, Wellington Rd, Clayton 3800, Australia*

<sup>b</sup>*Monash Centre for Synchrotron Science, Monash University, Wellington Road, Clayton 3800, Australia*

<sup>c</sup>*CLRC Daresbury Laboratory, Warrington WA4 4AD, UK*

<sup>d</sup>*Department of Physics, The University of Liverpool, Liverpool L69 7ZE, UK*

Available online 27 November 2006

## Abstract

The SmartPET collaboration is investigating the use of two planar high-purity germanium double-sided strip detectors as a Compton imaging positron emission tomography system. Monte Carlo simulations suggest that a large proportion of interactions within the detectors will occur within a small spatial volume, introducing significant ambiguities within the position and energy measurements made by the detectors. Under certain circumstances, the ambiguities will result in multiple interactions being detected as a single interaction. This investigation studied the effect of such multiple occupancies and found that approximately 45% of 511 keV events include multiple interactions within a  $5 \times 5 \times 20 \text{ mm}^3$  volume. Nevertheless, the effect on the quality of the final data remains quite acceptable.

© 2006 Elsevier B.V. All rights reserved.

PACS: 29.40.Gx; 87.62; 78.70

Keywords: Compton imaging; Orthogonal strip detector; Positron emission tomography

## 1. Introduction

The SmartPET collaboration is investigating the efficacy of using coplanar position and energy sensitive detectors as a combined Positron Emission Tomography (PET) and Compton imaging system for small-animal emission tomography studies [1].

PET utilizes coincident detections of collinear  $\gamma$ -rays emitted during a positron–electron annihilation to back-project lines of response (LoR) through the points on which the annihilation occurred, into the image space. Compton imaging utilizes kinematics to introduce angular resolution into the imaging system. Unlike PET or single photon emission computed tomography (SPECT) which both rely on LoRs, Compton imaging resolves the possible  $\gamma$ -ray origin to a cone of response (CoR) [2]. The determination of a CoR requires that an incident  $\gamma$ -ray undergo multiple inelastic interactions within the detector volume, and the location and energy deposit of each

interaction be measured. In simple reconstruction algorithms, the back-projected cone axis is described by the vector connecting the first and second interaction locations while the half-angle of the cone is determined from the energy deposited in the first interaction. It is planned to use a combination of Compton imaging and PET to decrease the number of false LoR back-projections and increase the efficiency and versatility of emission tomography [3].

## 2. Position resolution in the SmartPET detectors

The SmartPET detector system comprises two high-purity germanium (HPGe) orthogonal-strip detectors, each with an active area of  $60 \times 60 \times 20 \text{ mm}^3$  and a 5 mm strip pitch, as shown in Fig. 1(a). These facilitate the measurement of the location and energy deposit of individual  $\gamma$ -ray scatter/absorption interactions within the detector's volume.

Position resolution in the plane of an HPGe strip detector is obtained via readout of orthogonal electrode strips on either side of the detector. When a  $\gamma$ -ray interacts

\*Corresponding author. Tel.: +613 9905 9765; fax: +613 9905 3637.

E-mail address: [toby.beveridge@sci.monash.edu.au](mailto:toby.beveridge@sci.monash.edu.au) (T.E. Beveridge).

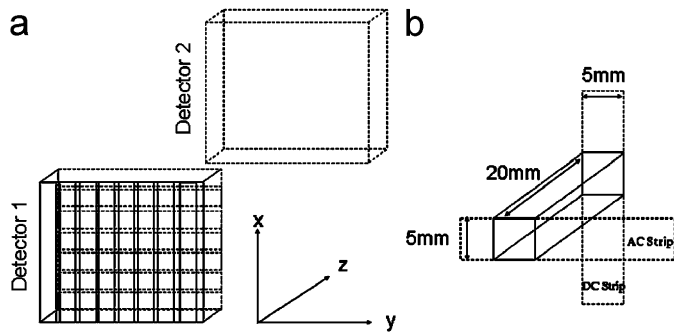


Fig. 1. (a) The SmartPET imaging system, (b) a detector element.

within the detector volume, the intersection of the two triggered strips defines the  $x$ - $y$  location of the interaction. Using this technique alone results in a position resolution defined by the strip pitch; however, this can be improved upon using digital processing techniques and interpolation of the signals on neighbouring strips [4].

The third dimension (depth) measurement is performed by analysing the pulse shape, which varies as a function of depth due to the time difference between the electron and hole clouds reaching the electrodes on opposite sides of the detector.

### 3. Incorrect detection of multiple occupancy

For the purposes of this discussion we define a single detector element as the  $5 \times 5 \times 20 \text{ mm}^3$  volume contained between the intercept of two orthogonal strips, see Fig. 1(b). For simultaneous multiple interactions within a detector element (multiple occupancy), resolving individual interactions may be complicated. Depending upon the depth separation of the interactions, there are three possible outcomes:

1. the interactions are resolvable;
2. the occurrence of multiple interactions is apparent but the individual interactions are irresolvable; or
3. the interactions are detected as a single interaction.

In case 1 or 2, the event can be included or excluded from the data set as warranted. Case 3 however, will result in incorrect information being passed to the reconstruction algorithm. The depth separation under which multiple interactions are indistinguishable from a single interaction will be referred to as the depth threshold for the remainder of this paper.

For simplicity, in the current analysis we have assumed that multiple interactions falsely detected as a single interaction will yield a detected energy deposit which is the combined sum of all the interactions and the detected location will be the energy-weighted displacement centre given by

$$\bar{x}_{\text{det}} = \frac{1}{E_T} \sum_i \bar{x}_i E_i$$

where  $x_{\text{det}}$  is the detected location,  $E_T$  is the total energy deposited, and  $x_i$  and  $E_i$  are the location and energy deposit of the  $i$ th interaction.

There are two classes of incorrect detections: those where the bad information includes the initial interaction and those where the initial interaction is detected correctly but a subsequent interaction is incorrectly detected. The distinction is important for cone back-projection since in the first case the energy used to determine the half-angle of the back-projected cone will be incorrect, whereas in the second case the effect is to only shift the cone axis.

### 4. Distinguishing multiple from single interactions

Geant 4 [5] Monte Carlo simulations were conducted to determine how often multiple occupancy occurs for a single annihilation/decay event. The initial simulation consisted of an isotropic  $\gamma$ -ray source situated 5 cm from the centre of the face of one of the SmartPET detectors, simulating the SPECT capability. For multiple occupancy to occur, there must be multiple interactions, and of interest is the fraction of those events that display multiple occupancy. Fig. 2 shows the fraction of events involving two or more interactions within the entire detector volume that include multiple occupancy. As the incident energy increases, the proportion of multiple occupancy events decreases. However even at 511 keV, over 45% of multiple interaction and hence back-projection-suitable, events have multiple occupancy.

Since the SmartPET system is primarily for PET studies, the following simulations model a 511 keV collinear point source, situated in the centre of the field-of-view with the two detectors separated by 10 cm. The definition of back-projection-suitable events was broadened to include events suitable for LoR reconstruction. Fig. 3 shows the fraction of events that include bad detections, for varying depth thresholds. The condition for an event to be considered bad

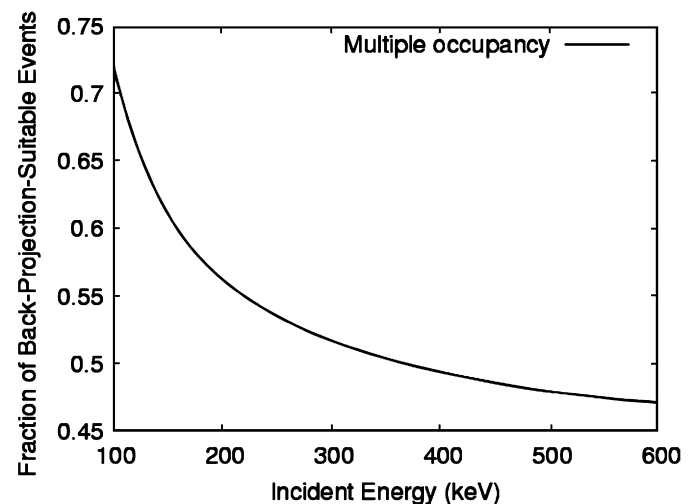


Fig. 2. The fraction of multiple interaction events that include multiple occupancy.

was for it to have multiple occupancy with a depth separation less than the depth threshold. Interestingly, the fraction of events including bad detections plateaus after a depth threshold of 4 mm. The reason is the geometry of the system and the fraction of coincident, single interaction, detections.

**5. Effect of false interactions on data quality**

In order to determine how these bad events affect the quality of the data set, we use the distance function, which is the distribution of closest approach of each back-projection to the true source location; as utilized by Wilderman et al. [6]. The data generated for Fig. 3 was sorted into two classes; good events containing no bad detections and bad events containing at least one bad detection. The results are shown in Fig. 4. The simulation assumed a depth threshold of 1 mm. The apparent energy and location of the bad detections was determined and back-projections calculated accordingly. Perfect spatial resolution and zero detector noise were assumed but

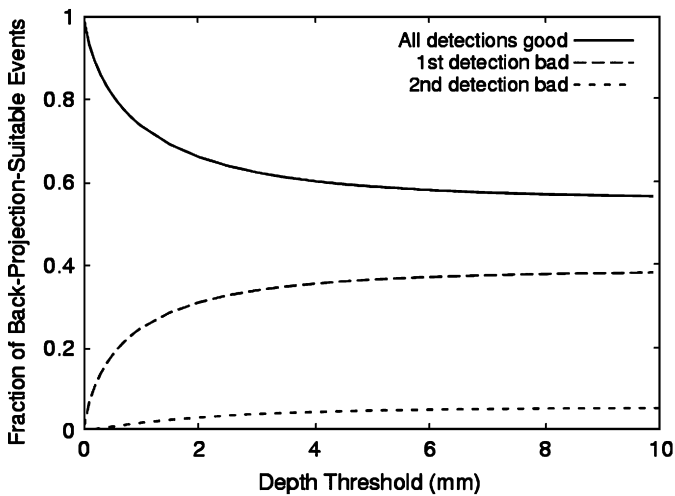


Fig. 3. The fraction of back-projection-suitable events that will include bad detections, for different depth thresholds.

Doppler broadening within the detectors was included. Doppler broadening dominates the energy uncertainty for moderate HPGe spectral resolution and accounts for the imperfect CoR distance function for good events shown in Fig. 4. The possibility of  $\gamma$ -tracking (attempting to determine the first interaction from kinematics) was not included and for cone back-projection this offers another level of discrimination. Similarly, no LoR validation techniques were applied and no discrimination based on the separation of detected interactions [7], or on scattering angle [3] was conducted.

**6. Discussion**

The broadening observed in the CoR distance function due to bad events, as shown in Fig. 4, is minimal. This is primarily due to the number of bad detections that cause a dual interaction to be detected as a single. Reconstruction is not possible with such events and they do not contribute to the distance function and so only 16% of events in the CoR distance function include bad detections. In addition, as mentioned in Section 3, for bad detections with three or more interactions, there are two possible scenarios. If the initial interaction is incorrectly detected, the energy used to determine the cone half-angle will be wrong and introduce a large error. However, if the first interaction is correctly detected, the cone axis is shifted by a small amount. The second scenario is the more likely, as the energy of the  $\gamma$ -ray is reduced after each interaction, and so the interaction cross-section of the material increases.

In the LoR case, the effect on the distance function is more pronounced. The broadening of the distance-function for good events in Fig. 4 is due to scatter within the air, elastic interactions and back-scatter from the opposing detector. The simulations are for perfect position resolution but the expected value for SmartPET is  $\sim 1$  mm FWHM which will lead to a considerably broader distance function for good events. Consequently, the bad detection induced broadening in excess of 1 mm is the primary concern. The bad events for LoRs are 25% of the total

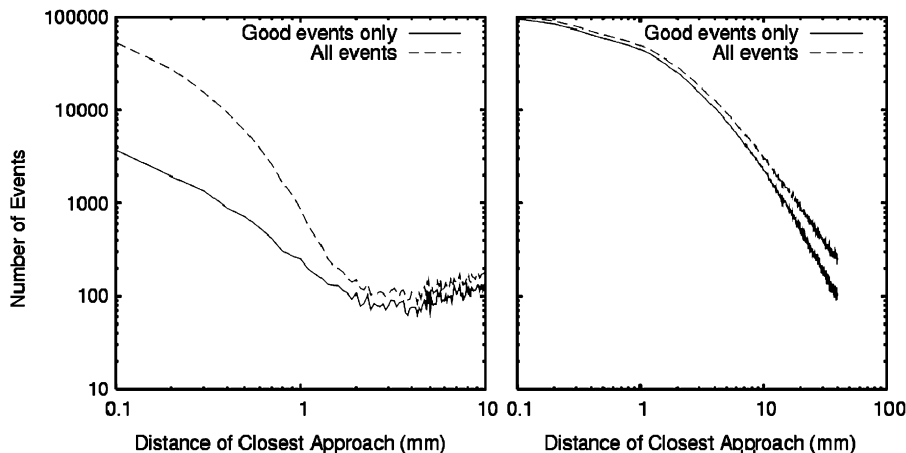


Fig. 4. The distance function for just the good events and all events for a 1 mm depth-threshold for LoRs (left) and CoRs (right).

however only 0.3% result in an error greater than 1 mm. The effect of bad detections on the distancefunction of the SmartPET system is therefore expected to be minimal.

## 7. Conclusion

It was found that a large fraction (45% at 511 keV) of back-projection suitable events in SmartPET will include multiple occupancy. However the three-dimensional position resolution combined with the system geometry means that bad detections will not introduce an unmanageable uncertainty into the data.

## Acknowledgements

TB acknowledges a School of Physics JL Willam Scholarship and a Monash Dean's Scholarship, and the

SmartPET collaboration (Medical Research Council Grant No 62861).

## References

- [1] C.J. Hall, P.J. Nolan, A.J. Boston, et al., A gamma tracking detector for nuclear medicine, *IEEE Nucl. Sci. Symp. Conf. Rec.* (2003).
- [2] G.W. Phillips, *Nucl. Instr. and Meth. B* 99 (1995) 674.
- [3] J.E. Gillam, T.E. Beveridge, R.A. Lewis, *IEEE Med. Image Conf. Rec.* (2004).
- [4] L. Mihailescu, W. Gast, R. Lieder, *IEEE Nucl. Sci. Symp. Conf. Rec.* (2002).
- [5] S. Agostinelli, Geant4 Collaboration, et al., *Nucl. Instr. and Meth. A* 506 (2003) 250.
- [6] S.J. Wilderman, et al., *IEEE Trans. Nucl. Sci. NS-44* (2) (1997).
- [7] C.E. Ordonez, W. Chang, A. Bolozdynya, *IEEE Trans. Nucl. Sci. NS-46* (4) (1999).